JOURNAL OF GEOPHYSICAL RESEARCH: OCEANS, VOL. 118, 1–15, doi:10.1029/2012JC008234, 2013

Shoaling of the nutricline with an increase in near-freezing temperature water in the Makarov Basin

Shigeto Nishino,[1] Motoyo Itoh,[1] William J. Williams,[2] and Igor Semiletov[3]

Received 28 May 2012; revised 3 September 2012; accepted 2 November 2012.

[1] The water mass changes in the Makarov Basin and adjacent areas associated with the recent loss of Arctic sea ice had not been studied in detail. We combined data obtained from multiple cruises in these regions and used chemical tracers to investigate the spatial and temporal changes in water masses. Our data show that a previously present temperature maximum water has disappeared from the Makarov Basin and Chukchi Abyssal Plain due to enhanced cooling and convection in the East Siberian Sea. In addition, a large volume of water has formed by cooling and convection and is flowing into the Makarov Basin, producing a temperature minimum with relatively high nutrients and resulting in a shoaling of the nutricline. This temperature minimum water likely originated from the eastern part of the East Siberian Sea, where significant open water areas appeared after 2005 in the freeze-up season. The water mass boundary between this temperature minimum water and the Pacific-origin temperature minimum water shifted westward from the Chukchi Plateau in the early 2000s to the Mendeleyev Ridge in the late 2000s, probably owing to a westward flow of the enhanced Beaufort Gyre associated with recent sea ice loss in the Canada Basin. Although the shoaling of the nutricline in the Makarov Basin could increase phytoplankton production, such production could decrease in the southern Makarov Basin because a large amount of sea ice meltwater covers that region and might decrease the nutrient supply from the subsurface layer.

Citation: Nishino, S., M. Itoh, W. J. Williams, and I. Semiletov (2013), Shoaling of the nutricline with an increase in near-freezing temperature water in the Makarov Basin, *J. Geophys. Res. Oceans*, *118*, doi:10.1029/2012JC008234.

1. Introduction

[2] In recent years, the Arctic has rapidly lost its summer sea ice cover [*Stroeve et al*., 2007; *Comiso et al*., 2008; *Kwok et al*., 2009]. The most catastrophic sea ice loss has been observed in the Pacific sector of the Arctic Ocean (western Arctic Ocean), where the spatial pattern of this ice loss has been well correlated with the spatial distribution of warm water from the Pacific Ocean [*Shimada et al*., 2006]. The loss of sea ice during summer increases the absorption of solar energy [*Perovich et al*., 2007] and changes properties of the surface water, such as the near-surface temperature maximum in the Canada Basin [*Jackson et al*., 2010]. In the winter freeze-up season, the surface water in the area of sea ice loss loses heat to the atmosphere. Sea ice then forms, accompanied by brine rejection and vertical convection. For example, the vertical convection in the polynyas in the Chukchi Sea [*Weingartner et al*., 1998; *Shimada et al*., 2005] and in the winter mixed layer in the eastern Arctic Ocean [*Shimada et al*., 2005; *Itoh et al*., 2007] could have formed the large volume water masses with high oxygen concentrations that have been found in the northern Chukchi Sea/southern Canada Basin and the northern Canada Basin, respectively. Because of recent losses of sea ice in summer and the subsequent thin and fragmented ice floes in winter, the wind can drive the ocean circulation more effectively. This has enhanced the Beaufort Gyre in the Canada Basin [*Shimada et al*., 2006; *Yang*, 2009], and as a result, more fresh water has accumulated within the Beaufort Gyre [*Proshutinsky et al*., 2009]. This deepens the nutricline, which may decrease phytoplankton production [*McLaughlin and Carmack*, 2010]. In this region, instead of vertical nutrient supply from the deepened nutricline to the euphotic zone, lateral transport of nutrients by eddies has become more important than previously. Nutrient transports by these eddies could impact the phytoplankton distribution [*Nishino et al*., 2011a]. Such eddies may appear more frequently because they are likely formed by baroclinic instability of the enhanced westward flow of the Beaufort Gyre associated with the recent loss of sea ice [*Kawaguchi et al*., 2012]. Much of our understanding of the effects of sea ice loss comes from measurements collected in the Canada Basin east of the Chukchi Plateau (see the topography given in Figure 1). In contrast, little is known about the water mass distributions

[1]Research Institute for Global Change, Japan Agency for Marine-Earth Science and Technology, Yokosuka, Japan.
[2]Institute of Ocean Sciences, Fisheries and Oceans Canada, Sidney, British Columbia, Canada.
[3]International Arctic Research Center, University of Alaska, Fairbanks, Alaska, USA.

Corresponding author: S. Nishino, Research Institute for Global Change, Japan Agency for Marine-Earth Science and Technology, 2-15 Natsushima, Yokosuka, Kanagawa 237-0061, Japan. (nishinos@jamstec.go.jp)

2169-9275/13/2012JC008234

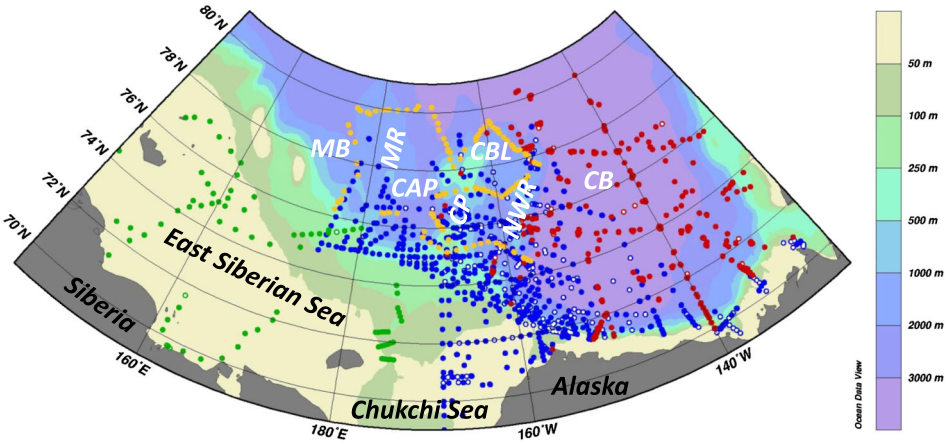

Figure 1. Map showing bathymetric features of the study area and locations of the hydrographic stations of the R/V *Mirai* cruises in 2002, 2004, 2008–2010 (blue); the CCGS *Louis S. St-Laurent* cruises from 2003 to 2010 (Canada/U.S. Beaufort Gyre Exploration Project; red); the USCGC *Polar Star* cruise in 2002 (Chukchi Borderland Project; yellow); and the cruise of Russian vessel *Yacob Smirniskyi* in 2008 (ISSS-08, International Siberian Shelf Study 2008; green). Closed circles indicate CTD and hydrographic water sampling stations; open circles indicate CTD observation stations. Geographical locations are abbreviated as follows: Canada Basin (CB), Northwind Ridge (NWR), Chukchi Plateau (CP), Chukchi Borderland (CBL), Chukchi Abyssal Plain (CAP), Mendeleyev Ridge (MR), and Makarov Basin (MB).

and their temporal changes in relation to the sea ice loss west of the Chukchi Plateau (i.e., the Chukchi Abyssal Plain and the Makarov Basin).

[3] The water mass distributions in the Canada Basin east of the Chukchi Plateau have been well studied. The upper part of the ocean is largely influenced by Pacific-origin water, which can be classified into two types based on seasonal modifications of the Chukchi Sea shelf: Pacific summer water (PSW) and Pacific winter water (PWW), which compose the upper halocline (depth < 200 m) and are characterized by a temperature maximum (S = 31–32, defined by the dimensionless practical-salinity-scale PSS-78 [UNESCO, 1981]; depth < 80 m) and a temperature minimum ($S \sim 33$; depth = 100–150 m) [*Coachman and Barnes*, 1961]. The PWW is also characterized by a nutrient maximum. In winter, minimal biological uptake of nutrients occurs in the Bering and Chukchi Seas [*Hansell et al*., 1993; *Codispoti et al*., 2005], and regenerated nutrients are added from the shelf sediments [*Jones and Anderson*, 1986]. The spreading of this nutrient-rich PWW into the Canada Basin maintains the nutrient maximum layer. Below the PWW lies the lower halocline water (LHW; $S \sim 34.2$, depth = 200 m), derived from shelf areas of the Atlantic sector of the Arctic Ocean, i.e., the eastern Arctic Ocean [*Aagaard et al*., 1981; *Jones and Anderson*, 1986] or basin areas of the eastern Arctic Ocean [*Rudels et al*., 1996; *Itoh et al*., 2007]. Deeper still, areas below the LHW are occupied by warm water originating from the Atlantic Ocean with a temperature maximum at 300–500 m depth.

[4] The PSW is further classified into Alaskan coastal water and Bering Sea water. The former is warmer, has a lower salinity, and is carried by a current along the Alaskan coast, whereas the latter is cooler, has higher salinity, and occupies the bulk of the central Chukchi Sea [*Coachman et al*., 1975]. *Shimada et al*. [2001] called the former eastern Chukchi summer water (ECSW) and the latter western Chukchi summer water (WCSW); we use this nomenclature to specify the season in which the waters pass through the Chukchi Sea shelf area. *Shimada et al*. [2001] also reported that ECSW is carried into the Canada Basin by the Beaufort Gyre and forms a temperature maximum at S = 31–32, which is significant east of the Chukchi Plateau. In contrast, WCSW seems to spread into the Chukchi Abyssal Plain west of the Chukchi Plateau, forming a temperature maximum around S = 32.5 (at least this was the case in the early 2000s) [*Shimada et al*., 2001; *Steele et al*., 2004]. Although this is the most well-known feature of the Pacific-origin water west of the Chukchi Plateau, basic characteristics such as its spatial and temporal variations are not clear.

[5] *Nishino et al*. [2008] studied the water mass distributions in the Chukchi Abyssal Plain by analyzing data obtained in the summer of 2004. They found that the temperature maximum of WCSW ($S \sim 32.5$) was sandwiched by two temperature minimum waters. The deeper temperature minimum water corresponded to PWW of $S \sim 33$. The shallower temperature minimum water ($S \sim 32$), which was fresher than PWW, was first reported in their study. Hereafter, this is referred to as fresh temperature minimum (frTmin) water. The frTmin water was supposed to be formed by cooling of the upper part of the WCSW during winter because the water there contained a large amount of sea ice meltwater. *Nishino et al*. [2008] also suggested that the Chukchi Plateau was a boundary between water masses, at least in the summer of 2004. The temperature minimum of frTmin water ($S \sim 32$) and the temperature maximum of WCSW ($S \sim 32.5$) were only found west of the Chukchi Plateau. In contrast, a larger volume of PWW was found east of the Chukchi Plateau compared to the west. Such differences in water masses could cause different responses of biological production to sea ice loss in summer [*Nishino et al*., 2011b]. In the Canada Basin east of the Chukchi Plateau, the enhancement of the Beaufort Gyre due to sea ice loss has deepened the nutricline and the nutrient-rich PWW as described above [*McLaughlin and Carmack*, 2010]. This, in turn, may have decreased

Table 1. Expedition Dates

Expedition	Month
Mirai 2002	2 September to 10 October 2002
2004	1 September to 12 October 2004
2008	26 August to 9 October 2008
2009	7 September to 15 October 2009
2010	2 September to 16 October 2010
LSSL 2003	7 August to 7 September 2003
2004	29 July to 2 September 2004
2005	29 July to 1 September 2005
2006	5 August to 14 September 2006
2007	26 July to 31 August 2007
2008	17 July to 21 August 2008
2009	17 September to 15 October 2009
2010	15 September to 15 October 2010
CBL 2002	19 August to 23 September 2002
ISSS 2008	15 August to 26 September 2008

biological production. In the Makarov Basin, which is located west of the Chukchi Plateau and outside the Beaufort Gyre, the nutricline is shallower than in the Canada Basin and nutrients are presumably supplied from shelf areas. Thus, biological production could increase there under improved light conditions with the disappearance of sea ice cover [*Nishino et al*., 2011b]. These studies shed light on the spatial variation in water masses and their influence on the biological response to summer sea ice loss. However, the origin, formation mechanism, and temporal changes of the water masses west of the Chukchi Plateau have not been well studied. In addition, it is not known how the temporal changes are related to the recent loss of sea ice. Changes in the characteristics of water masses transported into the Canada Basin through ocean circulation should also be clarified because such changes may affect biological production in the Canada Basin.

[6] Here we examine the temporal changes in frTmin water and WCSW west of the Chukchi Plateau and the association of these changes with the sea ice loss in the East Siberian Sea. The origin of the frTmin water is discussed using data from the East Siberian Sea. We also investigate the shift in the water mass boundary that appeared near the Chukchi Plateau in 2004. Furthermore, we examine the annual change in ocean circulation in the Canada Basin and the propagation of the upstream water mass changes into the basin. The biological responses to the changes in water mass distribution controlled by the ocean circulation are also discussed.

2. Data and Methods

[7] We combined the data obtained during cruises of the R/V *Mirai* in 2002, 2004, and 2008–2010; the CCGS *Louis S. St-Laurent* from 2003 to 2010 (Canada/U.S. Beaufort Gyre Exploration Project); the USCGC *Polar Star* in 2002 (Chukchi Borderland Project); and the Russian vessel *Yacob Smirniskyi* in 2008 (ISSS-08, International Siberian Shelf Study 2008). The expedition dates are summarized in Table 1. The data cover the Chukchi Sea, East Siberian Sea, Makarov Basin, and Canada Basin (Figure 1). The expeditions of the R/V *Mirai*, an ice-strengthened ship, were conducted during the time of the largest sea ice retreat (around mid-September) in the open water area of the western Arctic, especially focused on the western Canada Basin. The CCGS *Louis S. St-Laurent* cruises were carried out during summer in the central Canada Basin, and they especially focused on the Beaufort Gyre area [e.g., *Proshutinsky et al*., 2009]. Therefore, for the years when both cruises were conducted, the data cover wide areas of the Canada Basin. The data obtained a decade ago by the Chukchi Borderland Project are valuable to study temporal changes in water masses by comparison with the recent R/V *Mirai* data in the Chukchi Borderland area. The ISSS-08 cruise acquired data from an extensive area of the East Siberian Sea. Analysis of data collected by the Russian vessel *Yacob Smirniskyi*, R/V *Mirai*, and CCGS *Louis S. St-Laurent* allowed us to investigate the Siberian shelf-basin interaction and its influence to the Canada Basin.

[8] General descriptions of the R/V *Mirai* cruises are presented in the cruise reports [*Shimada*, 2002, 2004, 2008; *Kikuchi*, 2009; *Itoh*, 2010], which can be downloaded with the data from the Japan Agency for Marine-Earth Science and Technology (JAMSTEC) at http://www.godac.jamstec.go.jp/cruisedata/mirai/e/index.html. Data on the CCGS *Louis S. St-Laurent* cruises and some associated documents [e.g., *McLaughlin et al*., 2008, 2010] can be downloaded from the website of the Beaufort Gyre Exploration Project, Woods Hole Oceanographic Institution (http://www.whoi.edu/beaufortgyre/). Data on the USCGC *Polar Star* cruise in 2002 and the cruise report [*Woodgate et al*., 2002] can be downloaded from the Chukchi Borderlands website, Polar Science Center, Applied Physics Laboratory, University of Washington (http://psc.apl.washington.edu/CBL.html). *Anderson et al*. [2011] provided a detailed description of the collection methods of the ISSS-08 data [*Semiletov and Gustafsson*, 2009], and these data are available to the public upon request via the International Arctic Research Center (IARC) at http://www.iarc.uaf.edu/research/data.

[9] Using conductivity, temperature, depth (CTD) systems, data on temperature, salinity, oxygen, and chlorophyll-a (CTD-Chl) were acquired. The downloaded salinity and oxygen data were calibrated by comparing the raw data from the CTD systems to the bottled seawater data of salinity (analyzed using AUTOSAL salinometers) and oxygen (obtained by Winkler titration), respectively. The downloaded CTD-Chl data were not calibrated. In some stations, Chl-a concentrations of bottled seawater were measured using a fluorometric non-acidification method [*Welschmeyer*, 1994]. Both values were closely correlated. Furthermore, the basin-scale CTD-Chl distribution seems to be consistent with the nutrient distribution as described in section 3.6. The quality of CTD-Chl data was therefore good enough for a qualitative analysis of the basin-scale distribution.

[10] Data on nutrients, oxygen, and total alkalinity of bottled seawater were used in this study. These parameters were analyzed on board the research vessels: nutrients by continuous flow automated analytical systems [*Gordon et al*., 1993], oxygen by Winkler titration based on the WOCE Hydrographic Programme method [*Dickson*, 1996], and total alkalinity by potentiometric titration [*Haraldsson et al*., 1997; *Yao and Byrne*, 1998]. The total alkalinity values were calibrated against certified reference material provided by Dr. Dickson of the Scripps Institute of Oceanography. From these bottled seawater data, we calculated parameters of N*, NO, and the fraction of sea ice meltwater (f_{SIM}), as described below, to examine the characteristics of water masses and the water mass distribution.

[11] The parameter N* was defined following *Gruber and Sarmiento* [1997] and expressed as $N^* = 0.87([NO_3^-] - 16$

Table 2. End-Member Values Used in This Study

	Salinity	Total Alkalinity (μmol/kg)
SIM (sea ice meltwater)	4	263
OF (meteoric water, salinity deficit of Pacific water)	0	930
ATW (Atlantic water)	34.87	2306

$[PO_4^{3-}] + 2.9$) (μmol/kg). It refers to the nitrate deficit (negative values) or excess (positive values) with respect to phosphate. Under a process of denitrification, nitrate is used for organic matter decomposition instead of oxygen and is removed as free nitrogen gas from the water column, resulting in a decrease in N*. However, if nitrogen fixation occurs (the process by which nitrogen gas in the atmosphere is fixed into organisms in a water column), the N* value increases. The constant value 2.9 was used to make the global average of N* for the ocean zero, and the value of 0.87 was used to account for phosphate released by the regeneration of organic matter during denitrification. In the Chukchi Sea, significant denitrification occurs within shelf sediments [*Devol et al*., 1997; *Yamamoto-Kawai et al*., 2006]. Therefore, in water that has passed through the Chukchi Sea, N* decreases to negative values [*Codispoti et al*., 2005; *Nishino et al*., 2005]. In the Chukchi Sea, ammonium concentrations reach ~4 μmol/kg. Thus, it would be preferable to use the total nitrogen including ammonium instead of nitrate for the N* calculation [*Codispoti et al*., 2005; *Nishino et al*., 2005]. However, ammonium data were not always obtained in the cruises described above. If we use total nitrogen for the N* calculation, the N* values are ~70% of those calculated from nitrate in the Chukchi Sea. These values are still smaller than those in the basin areas. In the basin areas, ammonium concentrations are nearly zero because there are almost no sources of ammonium and the ammonium is converted to nitrate through biological oxidation, i.e., nitrification. As a result, in the basin areas the ammonium concentrations are negligible for the N* calculation and N* can serve as an index of denitrification. Significant denitrification has occurred in the shelf sediments of the Chukchi Sea. Consequently, the spreading of low-N* water from the Chukchi Sea into basin areas can be traced by an N* minimum.

[12] The parameter NO was defined by *Broecker* [1974] and expressed as $NO = 9[NO_3^-] + [O_2]$ (μmol/kg). This parameter is a quasi-conservative tracer that is independent of biological processes in a layer isolated from the atmosphere. It is used to distinguish among water masses with different values of preformed nitrate and oxygen. For example, the water in the euphotic zone (where nitrate is consumed and oxygen is produced by photosynthesis) could lose oxygen to the atmosphere, decreasing NO. Conversely, in water that has experienced convection by surface cooling in winter, ventilation could increase the value of NO. In the Arctic Ocean, the LHW is characterized by a NO minimum, which is caused by photosynthesis and the outgassing of oxygen to the atmosphere in the shelf [*Jones and Anderson*, 1986] or basin [*Rudels et al*., 1996] areas of the eastern Arctic Ocean. *Wilson and Wallace* [1990] investigated the NO distribution in the shelf seas surrounding the Arctic Ocean and found that it was difficult to identify the source region of the NO minimum LHW. The shelf seas had widely ranging distributions of NO, most of which were centered on the low NO value of LHW. They also mentioned that the NO profile had a vertical maximum at the PWW layer in the central Arctic Ocean, suggesting that the water had undergone winter convection.

[13] We calculated the fraction of sea ice meltwater (f_{SIM}) from the relationship of total alkalinity and salinity based on the analysis by *Yamamoto-Kawai et al*. [2005]. Assuming that the seawater sample is a mixture of Atlantic water (ATW), sea ice meltwater (SIM), and other fresh water (OF) that includes river runoff, precipitation, and fresh water carried by Pacific water (PSW and PWW), which has lower salinity than Atlantic water, the fractions of each end-member can be calculated using the following mass balance equations:

$$f_{SIM} + f_{OF} + f_{ATW} = 1 \tag{1}$$

$$f_{SIM} S_{SIM} + f_{OF} S_{OF} + f_{ATW} S_{ATW} = S \tag{2}$$

$$f_{SIM} TA_{SIM} + f_{OF} TA_{OF} + f_{ATW} TA_{ATW} = TA. \tag{3}$$

[14] Here S and TA are the observed salinity and total alkalinity of seawater, respectively, and f, S, and TA with subscripts are the fraction, salinity, and total alkalinity, respectively, of the three end-members of SIM, OF, and ATW. Each end-member value is listed in Table 2. Although *Yamamoto-Kawai et al.* [2005] used $TA_{OF} = 831$ μmol/kg for the entire Arctic Ocean, we use $TA_{OF} = 930$, which is suitable for the western Arctic Ocean according to their analysis. The fraction of sea ice meltwater f_{SIM} increases, when seawater is influenced by sea ice melt in summer, and decreases, when seawater is influenced by sea ice formation in winter. A negative f_{SIM} implies that sea ice formation, which removes fresh water from and ejects brine into seawater, is dominant over sea ice melt.

3. Results

3.1. Temporal Changes in Water Masses in the Makarov Basin

[15] Although there have been few observations in the Makarov Basin, we can compare the data from the Chukchi Borderland cruise in 2002 [*Woodgate et al*., 2002] and the R/V *Mirai* cruise in 2008 [*Shimada*, 2008] to examine temporal changes in water masses that have not yet been closely studied (Figure 2). In 2002, research in the Makarov Basin was conducted in late August, 1 month earlier than the research in 2008. However, both studies were conducted during the season of greatest sea ice retreat (around mid-September) in the year. Therefore, we examine not seasonal but yearly changes between 2002 and 2008. The research area was covered by sea ice in 2002 but had open water in 2008. Because of the lack of sea ice in 2008, the surface water could absorb solar energy, resulting in warmer surface water than that in 2002 (Figures 2b and 2g). However, below the warm surface water in 2008, near-freezing water occupied depths of 25–100 m. The water there was colder than that in 2002. Warm water was found in 2002 at depths of 70–90 m south of 77°N, but was not found in 2008. These were not seasonal changes because the research period in 2008 was not a cooling phase and the warm water still existed at the surface. The

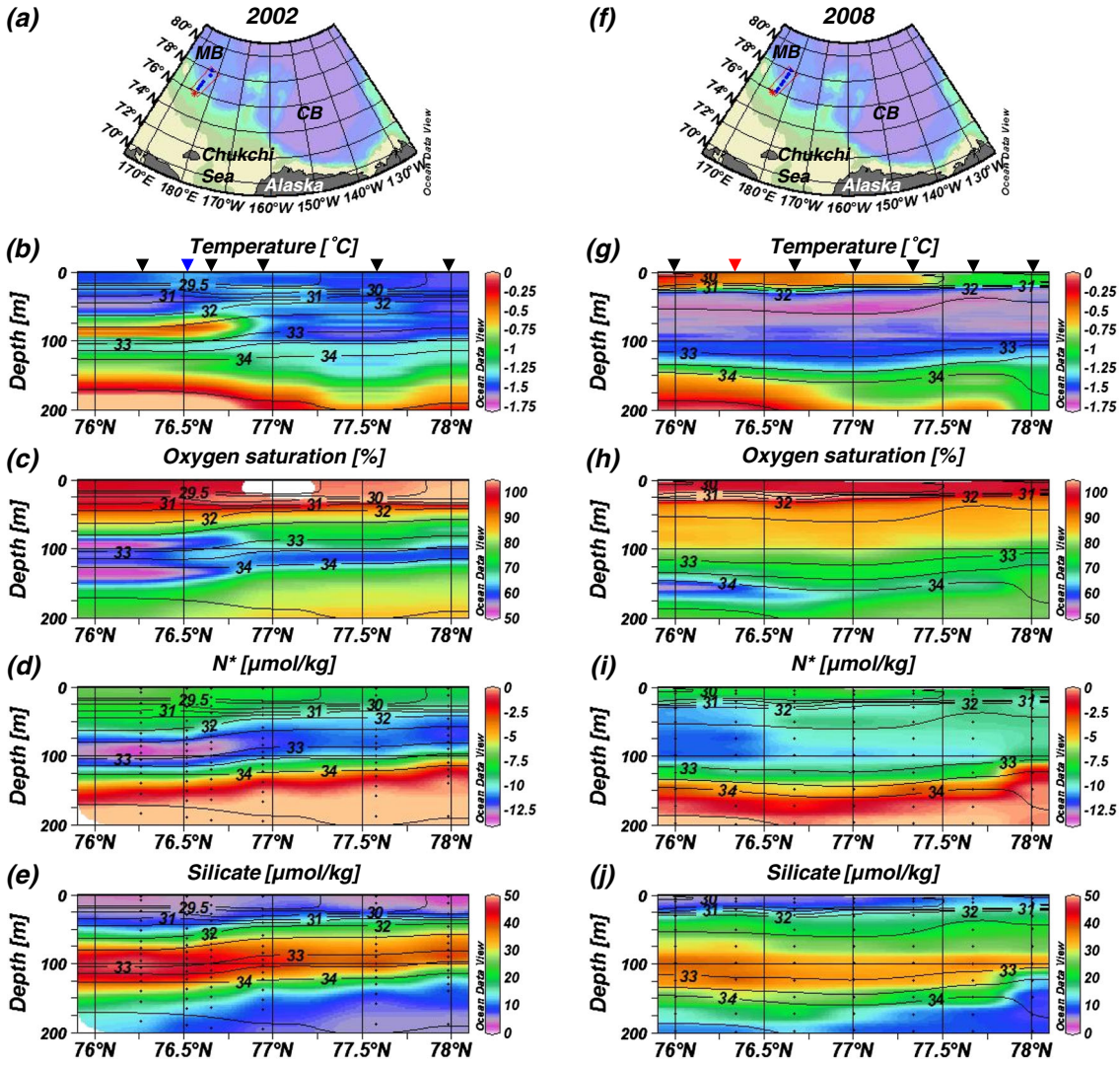

Figure 2. (a and f) Map of stations from the shelf slope to the interior of the Makarov Basin and (b and g) temperature (°C), (c and h) oxygen saturation (%), (d and i) N* (µmol/kg), and (e and j) silicate (µmol/kg) distributions in 2002 and 2008, respectively, along the observational line in each map of Figures 2a and 2f. Salinity contours are superimposed on each panel of the vertical section. In Figures 2b and 2g, the positions of the stations are indicated by inverse triangles. At stations denoted by blue and red inverse triangles, diagrams of the water properties are shown in Figure 3.

changes are thought to reflect different conditions of water mass formation in the different years. Here we analyze the water mass characteristics to understand their temporal changes, the disappearance of the warm water observed at 70–90 m in 2002, and the formation mechanism of cold water below the warm surface water in 2008.

[16] In 2002, a subsurface temperature maximum water around $S = 32.5$, which was thought to be WCSW [*Shimada et al.*, 2001], appeared to spread toward the basin south of 77°N (Figure 2b). The temperature maximum was sandwiched by two temperature minima, as described in section 1. However, the deeper temperature minimum, which was caused by the influence of the PWW, was not as prominent. This was because the Makarov Basin is distant from the source region of PWW, i.e., the Chukchi Sea. The distribution of oxygen saturation, which is a more useful parameter to estimate the degree of ventilation and biological decay than oxygen itself, was characterized by two minimum layers south of 77°N: one was between isohaline surfaces of $S = 32.5$ and 33 and the other was just below an isohaline surface of $S = 34$ (Figure 2c). The distribution of oxygen saturation was very similar to the oxygen distribution and the salinity values of both the minima of oxygen saturation and oxygen were the same. Therefore, for simplicity, we refer to the minimum of oxygen saturation as the "oxygen minimum." The water in the lower oxygen minimum layer was identified as oxygen-poor LHW [*Shimada et al.*, 2005], which was formed by decomposition of organic matter accumulated on shelf slope sediments west of the Chukchi Plateau [*Nishino et al.*, 2009]. The upper oxygen minimum layer corresponded to a N* minimum layer (Figure 2d). The N* minimum is a signal of water that has passed through the Chukchi Sea shelf, where significant denitrification occurs within the shelf sediments [*Devol et al.*, 1997; *Yamamoto-Kawai et al.*, 2006],

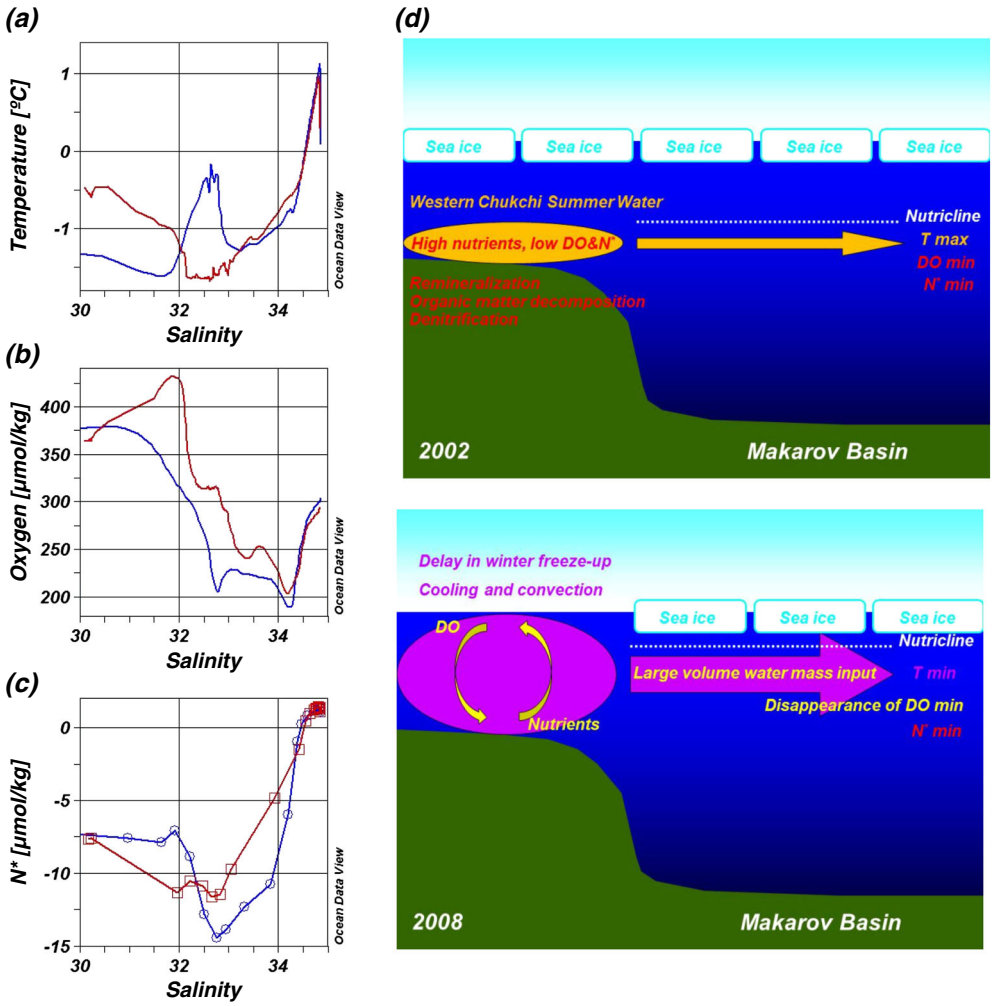

Figure 3. Diagrams of (a) temperature-salinity, (b) oxygen-salinity, (c) N*-salinity at almost the same stations in 2002 (blue) and 2008 (red), and (d) schematics of the change in water characteristics from 2002 to 2008. In Figures 3a–3c, the locations of the stations in 2002 (76°31.44′N, 175°51.82′E) and 2008 (76°20.26′N, 176°19.85′E) are indicated by the blue and red inverse triangles in Figures 2b and 2g, respectively.

leading to decreased values of N* [*Codispoti et al.*, 2005; *Nishino et al.*, 2005]. In other words, in the Chukchi Sea shelf, where WCSW occupies the bulk of the central area of the sea during summer, both organic matter decomposition and denitrification occur within the shelf sediments, and the diffusion of pore water from the sediments reduces oxygen concentrations and N* values in the bottom of the WCSW. This is consistent with the fact that the temperature profile was maximum at the core of the WCSW around $S = 32.5$, but the oxygen and N* profiles reached minima at a deeper level of $S = 32.8$ (Figure 3). The decomposition of organic matter (including the dissolution of hard parts) within the shelf sediments remineralizes nutrients (e.g., nitrate, phosphate, and silicate), which are supplied to the WCSW from the sediments. Hence, WCSW is characterized by nutrient-rich water, but the nutrient concentrations are lower than those of PWW around $S = 33$ (Figure 2e) [*Jones and Anderson*, 1986]. The spreading of WCSW into the Makarov Basin thus forms the temperature maximum around $S = 32.5$ and oxygen and N* minima around $S = 32.8$ with relatively high nutrient concentrations.

[17] Dramatic changes from 2002 to 2008 were observed in the distributions of physical and chemical characteristics of the water in the Makarov Basin (Figures 2 and 3). In 2008, WCSW disappeared and a large-volume water mass of near-freezing temperature with a salinity range of 32.2–32.8 occupied the Makarov Basin (Figures 2g and 3a). The subsurface ($S = 32.2$–32.8) oxygen saturation in 2008 (~85%) was higher than that in 2002 (<60%), and there was no upper oxygen minimum layer in 2008 (Figures 2h and 3b). The water characteristics of near-freezing temperature, the higher oxygen saturation, and the larger volume of the layer of $S = 32.2$–32.8 in 2008 compared to those in 2002 suggest that the water occupying the layer of $S = 32.2$–32.8 in 2008 would have been formed by winter cooling and convection as discussed by *Shimada et al.* [2005] for the cold, thick, and oxygen-rich PWW in the southern Canada Basin. Such water mass formation has become more likely in shelf areas in recent years because of the significant delays in winter freeze-up [*Markus et al.*, 2009]. The winter convection in the shelf areas in 2008 may have been strong enough to collapse the characteristics

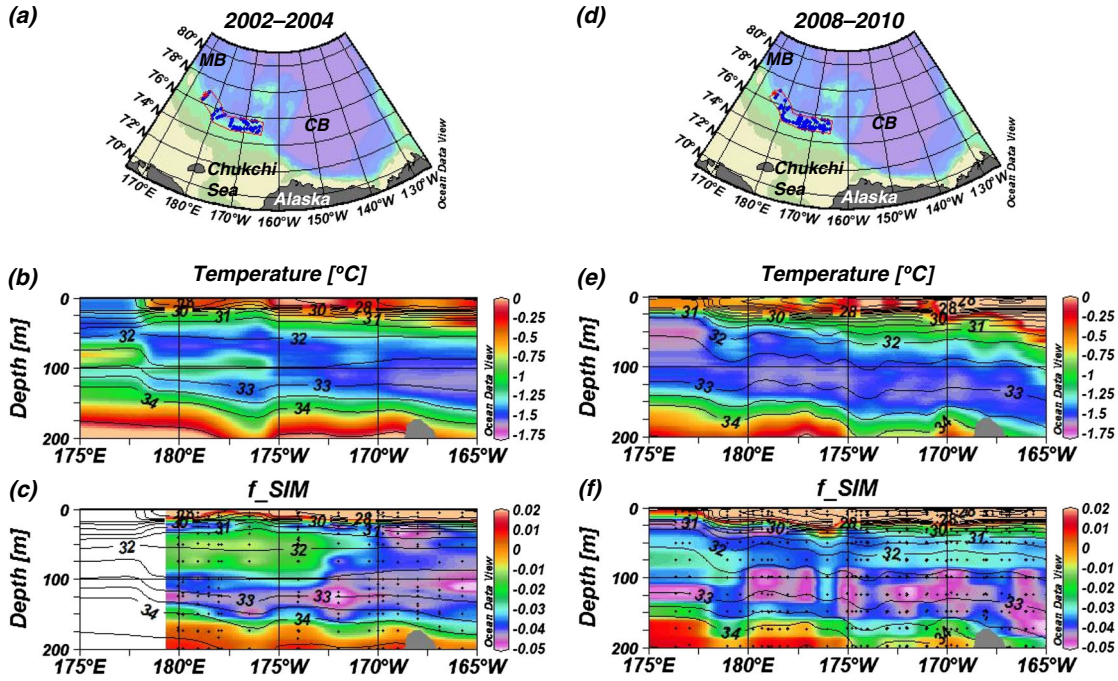

Figure 4. (a and d) Map of stations along a shelf slope from 175°E to 165°W and (b and e) temperature (°C), and (c and f) f_{SIM} distributions in vertical sections along the shelf slope in 2002–2004 and 2008–2010, respectively.

of the WCSW, such as the temperature maximum and oxygen minimum, resulting in the disappearance of the WCSW in the Makarov Basin. The schematics of the change in water characteristics are shown in Figure 3d. The water of $S = 32.2$–32.8 south of 76.5°N in 2008 was also characterized by a N* minimum (Figures 2i and 3c), but the value of N* at the minimum was higher than that observed in 2002. This suggests that the water was derived from the shelf area but was well mixed vertically by winter convection. Ammonium (>0.5 mol/kg) was detected in the near-freezing and N* minimum water of $S = 32.2$–32.8 south of 76.5°N (data not shown). The concentration of ammonium in the basin area in winter is likely zero owing to nitrification, as suggested by *Whitledge et al*. [1986] in their research on the Bering Sea. Therefore, the near-freezing temperature water with ammonium is not formed in the Makarov Basin in winter. Rather, the water undergoes winter convection in the shelf area and remains until summer when the ammonium is supplied from the shelf sediments. Then the water spreads into the Makarov Basin south of 76.5°N during the summer. Simultaneously, the water remaining on the shelf until summer would decrease oxygen saturation during winter from a saturated level to the observed level of ~85%. It would also increase nutrient concentrations by biological processes within the shelf sediments. Owing to this inflow of a large-volume water mass of $S = 32.2$–32.8 with high nutrient concentrations, the nutricline in the Makarov Basin just above this water mass (i.e., just above the $S = 32.2$ isohaline surface) would become shallower, as observed in 2008 (Figure 2j). It is notable that the nutricline is deepening in the Canada Basin because of the accumulation of fresh water within the wind-driven Beaufort Gyre [*McLaughlin and Carmack*, 2010], whereas the nutricline in the Makarov Basin is shoaling because of the buoyancy-driven inflow described above.

3.2. Temporal Changes in Water Masses Along the Shelf Slope

[18] As described in section 1, an east-west water mass boundary was found around the Chukchi Plateau in 2004. The frTmin water and WCSW were only found west of the Chukchi Plateau; a larger volume of PWW occupied the area east of the Chukchi Plateau than the area west of the plateau [*Nishino et al*., 2008]. Here we examine the temporal changes in water masses along the shelf slope to investigate the boundary shift.

[19] At least until 2004, we observed the temperature maximum of WCSW west of the Chukchi Plateau. However, in 2005–2007, we collected no data in that region. After 2008, the WCSW was no longer observed there, as described above. Therefore, we compared the data between the periods 2002–2004 (Figures 4a–4c) and 2008–2010 (Figures 4d–4f) along the shelf slope across the Chukchi Plateau. We observed the temperature distribution (Figures 4b and 4e) that characterizes each water mass (frTmin water, WCSW, and PWW). However, from the temperature distribution alone, it is difficult to examine the differences in the temperature minima of the frTmin water and PWW. Useful information to distinguish the waters was derived from freshwater distributions. We calculated the fractions of sea ice meltwater (f_{SIM}) from the relationship of total alkalinity and salinity based on the analysis by *Yamamoto-Kawai et al*. [2005] (Figures 4c and 4f).

[20] In 2002–2004, there was a temperature maximum of WCSW around $S = 32.5$ west of 175°W and a temperature minimum of PWW around $S = 33$, which was prominent east of 170°W near the Chukchi Plateau (Figure 4b). Furthermore, west of 175°W, a temperature minimum was centered on $S = 32$ above the temperature maximum of WCSW. The

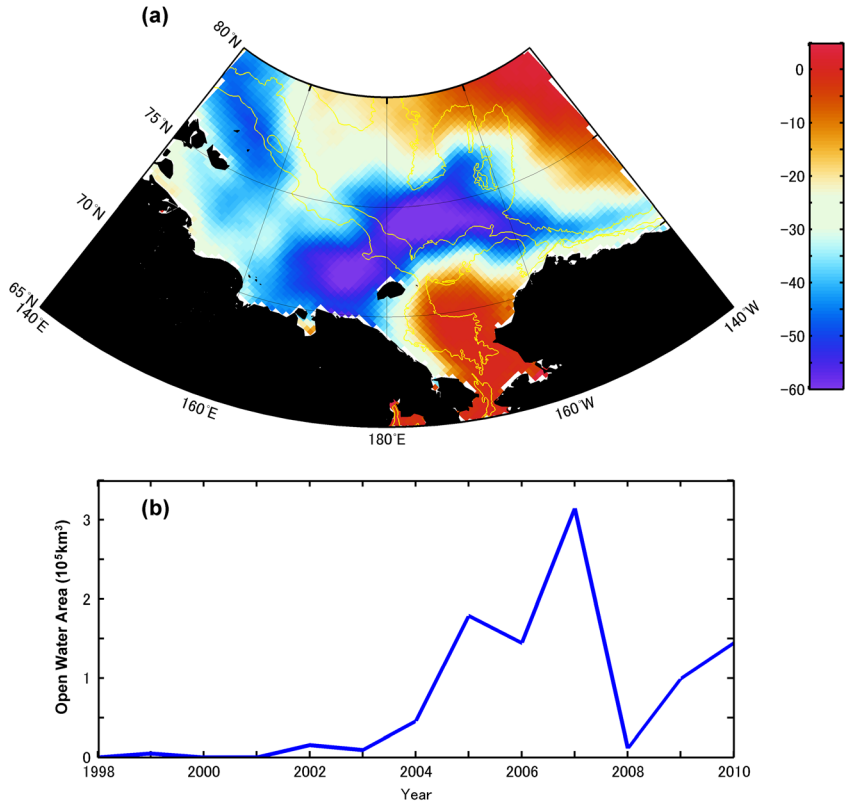

Figure 5. (a) Differences in Arctic sea ice concentration (%) in October between the low ice phase (2005–2010) and a long-term mean (1979–2004), and (b) the open water area (10^5 km^3), defined as an area where the sea ice concentration is less than 15%, in the region between 160°E and 180° and south of the 50 m isobath during 1998–2010. Data were generated from Special Sensor Microwave/Imager (SSM/I) observations using the NASA Goddard algorithm [*Comiso et al*., 2008] and were archived by the National Snow and Ice Data Center (NSIDC). In Figure 5a, yellow contours indicate isobaths of 50, 100, and 2000 m.

origin of this temperature minimum was different from that of PWW ($S \sim 33$), although both were likely formed by winter convection. *Nishino et al*. [2008] used the f_{SIM} distribution to distinguish the origins of these waters. The distribution indicated that PWW was characterized by a vertical minimum of f_{SIM} with large negative values. This suggested that the water was strongly influenced by brine rejection in winter (Figure 4c). Although the PWW seemed to be confined east of 170°W, based on the temperature distribution, a thin f_{SIM} minimum layer extended west of 170°W. This indicated that the PWW also spread west of 170°W, but only a little. In contrast, the coldest water around $S = 32$ west of 175°W had a vertical maximum of f_{SIM} with small negative values. This near-zero value of f_{SIM} implied a net balance between sea ice melt (positive) and sea ice formation (negative). This suggests that the water containing sea ice meltwater in summer experienced brine rejection in winter, or that significant sea ice melt and brine rejection did not occur. The latter scenario may be unrealistic on the shelf. Below this temperature minimum, around $S = 32$, a temperature maximum of WCSW always appeared. Therefore, the temperature minimum was likely caused by winter convection in the upper part of the WCSW, which may have large amounts of sea ice meltwater. This was referred to as frTmin water [*Nishino et al*., 2008]. The temperature maximum of WCSW around $S = 32.5$ would correspond to the lower part of the water that was not influenced by winter convection and cooling from the sea surface.

[21] Furthermore, we newly analyzed the vertical sections of temperature and f_{SIM} in 2008–2010. In 2008–2010, the western boundary of the prominent temperature minimum of PWW around $S = 33$, which was found roughly at 170°W near the Chukchi Plateau in 2002–2004, moved westward to 180°E near the Mendeleyev Ridge (Figure 4e). Likewise, the western boundary of the thick and prominent f_{SIM} minimum layer around $S = 33$ was also found at 180°E in 2008–2010 (Figure 4f). West of 180°E (west of the Mendeleyev Ridge), there was a new type of water with a temperature minimum around $S = 32.5$. On the basis of only the temperature distribution, it would be difficult to identify this water as the frTmin water or PWW. This temperature minimum water was also characterized by an f_{SIM} maximum of around $S = 32.5$, which is obviously different from the f_{SIM} minimum of PWW of around $S = 33$. As described above, the large values of f_{SIM} around $S = 32.5$ suggest that the water might have originally been WCSW that contained a large amount of sea ice meltwater in summer and then experienced winter convection over the shelf area, before spreading to the shelf slope and basin areas. Enhanced cooling of the water column in the shelf area probably collapsed the characteristic temperature maximum of the WCSW. Therefore, the temperature minimum water of $S \sim 32.5$ could be classified as the frTmin

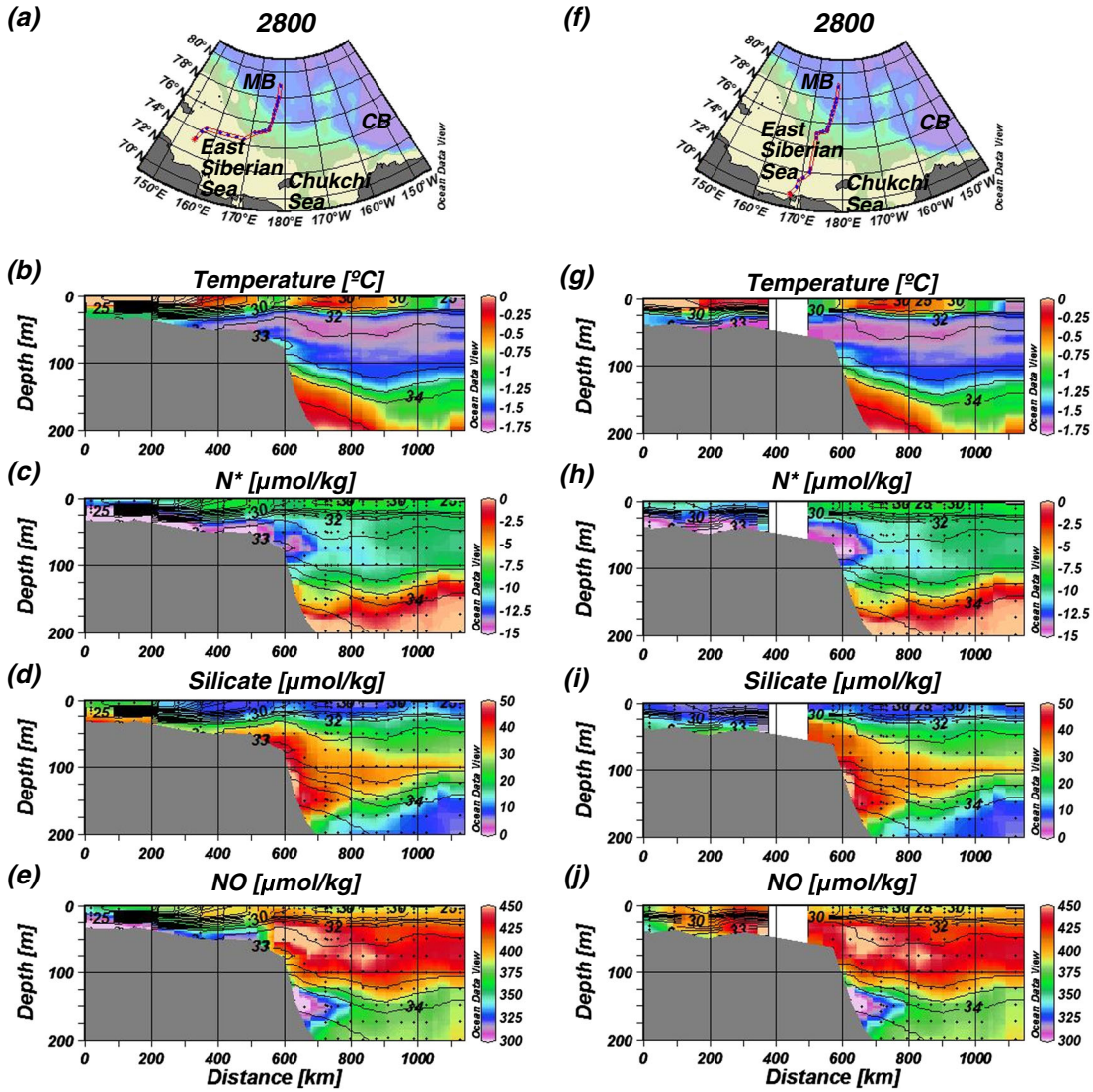

Figure 6. (a and f) Map of stations and (b and g) temperature (°C), (c and h) N* (µmol/kg), (d and i) silicate (µmol/kg), and (e and j) NO (µmol/kg) distributions in vertical sections along observational lines from the western and eastern parts of the East Siberian Sea, respectively, to the Makarov Basin in 2008.

water. The eastern boundary of the frTmin water also moved from 170–175°W to 180°E. The westward migration of these water masses may be consistent with an enhanced Beaufort Gyre and westward flow along the shelf slope. We discuss this point further later in this paper.

3.3. Sea Ice Distribution in the Early Freeze-Up Season

[22] The disappearance of WCSW and the appearance of cold, thick, and oxygen-rich water around $S \sim 32.5$ in the Makarov Basin could be associated with winter cooling and convection in shelf areas, where the significant delays in winter freeze-up could have caused the latter water to form more frequently. To identify where this water could have formed before the winter freeze-up, we examined the sea ice distribution in October, when the surface water cooling begins. We calculated differences in Arctic sea ice concentration between the low ice phase (2005–2010) and a long-term mean (1979–2004) in October (Figure 5a). The sea ice concentration was greatly reduced during the recent low ice phase in the eastern part of the East Siberian Sea and the Chukchi Sea shelf slope at 180–160°W, 73–75°N. Therefore, these two regions are possible sites where the cold, thick, and oxygen-rich water around $S \sim 32.5$ formed more frequently in recent years. However, the data along the shelf slope in 2008–2010 (Figures 4e and 4f) suggest that there was no WCSW with $f_{SIM} > 0$ to be changed into cold water with $f_{SIM} \sim 0$ by cooling and convection with sea ice formation (brine rejection) around the Chukchi Sea shelf slope. Instead, the layer around $S = 32.5$ was occupied by PWW. In addition, the water that formed in the Chukchi Sea shelf slope would have difficultly contacting the shelf sediments, where denitrification decreases the N* value and ammonium is supplied to the bottom water in the following summer. Therefore, this water could not have the characteristics found in Makarov Basin, which had cold, thick, and oxygen-rich water with $S \sim 32.5$, a N* minimum, and ammonium concentrations of >0.5 µmol/kg. Such properties could be found in the eastern part of the East Siberian Sea.

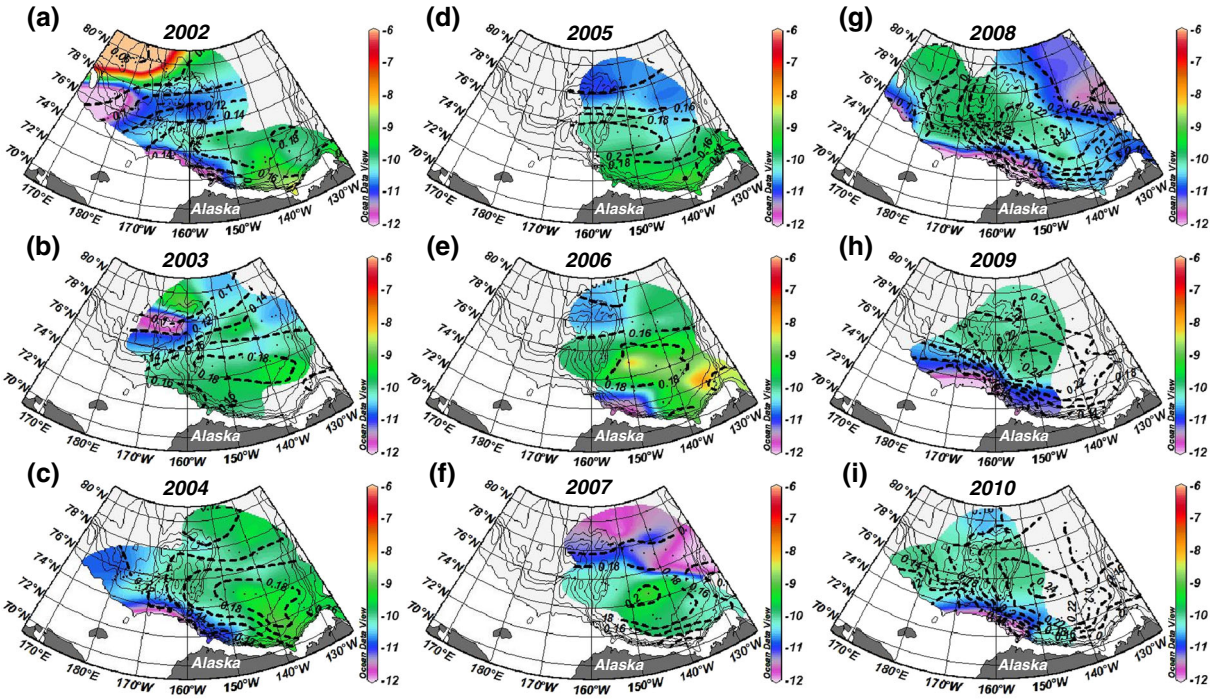

Figure 7. Dynamic height (dyn m) at 100 m relative to 250 m (dashed contours) and N* (μmol/kg) at an isohaline surface of $S = 32.8$ (colors) in (a) 2002, (b) 2003, (c) 2004, (d) 2005, (e) 2006, (f) 2007, (g) 2008, (h) 2009, and (i) 2010.

[23] We also calculated the open water area (<15% of sea ice concentration) in October in the eastern part of the East Siberian Sea (160°E–180°, depth < 50 m) from 1998 to 2010 (Figure 5b). In this region, there were almost no open water areas before 2004, but after 2005, extensive open water areas appeared, except in 2008. This is consistent with the water mass changes in the Makarov Basin. Before 2004, sea ice covered the East Siberian Sea in October, and because of the sea ice cover the WCSW did not lose heat to the atmosphere. The spread of the water into the Makarov Basin could therefore have formed the temperature maximum of the WCSW. However, after 2005 an extensive area of open water occurred in October in the eastern part of the East Siberian Sea, allowing for heat loss from the WCSW to the atmosphere and resulting in the formation of cold, thick, oxygen-rich water by cooling and convection.

3.4. Origin of Fresh Temperature Minimum Water

[24] The frTmin water around $S = 32$ in 2002 and $S = 32.5$ in 2008 could have been formed by modification of the WCSW through winter cooling and convection in the shelf areas, where the winter freeze-up has been significantly delayed recently. The frTmin water, like the WCSW, seemed to spread from the East Siberian Sea rather than the Chukchi Sea, as shown in the water mass distributions along the shelf slope (Figure 4). In addition, the eastern part of the East Siberian Sea is a plausible site for the WCSW modification to form frTmin water by cooling and convection. There, the area of open water in the winter freeze-up season has recently expanded (Figure 5b). However, in the East Siberian Sea, there are little hydrographic data with which to study the origin of frTmin water. In 2008, an extensive observational cruise was conducted in the Siberian shelf seas as part of the International Siberian Shelf Study (ISSS-08) [*Semiletov and Gustafsson*, 2009; *Anderson et al.*, 2011]. To specify the source region of frTmin water from the hydrographic data, we compared two sections by combining the ISSS-08 data with the R/V *Mirai* data collected in 2008. One section was from the western part of the East Siberian Sea to the Makarov Basin, and the other section was from the eastern part (Figure 6).

[25] The frTmin water around $S = 32.5$ in the Makarov Basin seemed to spread from the western part of the East Siberian Sea (Figure 6b). At the bottom of the shelf, there was extremely low-N* water (Figure 6c). This low-N* water may have come from the Chukchi Sea. Its N* concentration could have been further reduced by contact with the shelf sediments of the East Siberian Sea, where significant denitrification may occur [*Codispoti and Richards*, 1968; *Wilson and Wallace*, 1990]. The low-N* signal appeared to spread into the Makarov Basin with the frTmin water. The frTmin water also had high nutrient (e.g., silicate) concentrations at the bottom of the shelf, and this water appeared to carry high nutrient concentrations into the Makarov Basin (Figure 6d). However, the NO values of the water were quite different between the shelf and the basin (Figure 6e). The NO of bottom shelf water in the western part of the East Siberian Sea was extremely low compared to that of frTmin water around $S = 32.5$ in the Makarov Basin. The low NO of the bottom shelf water resulted from the decomposition of terrestrial organic matter derived from Russian rivers, with low nutrients compared to marine organic matter [*Semiletov et al.*, 2005; *Anderson et al.*, 2011]. However, the high NO of the frTmin water around $S = 32.5$ in the Makarov

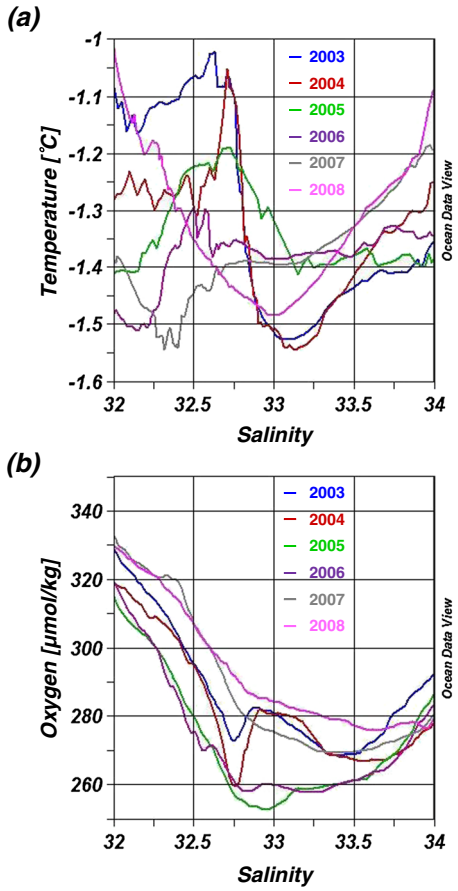

Figure 8. Temporal variation in (a) temperature (°C) and (b) oxygen (µmol/kg) profiles with respect to salinity from 2003 to 2008 at 79°N, 150°W.

Basin was caused by winter convection increasing the preformed oxygen in the water. Therefore, this water could not have been derived from the western part of the East Siberian Sea.

[26] In the eastern part of the East Siberian Sea, the bottom shelf water was near freezing and may have spread into the Makarov Basin to form the temperature minimum of frTmin water around $S = 32.5$ (Figure 6g). This water accompanied the N* minimum layer (Figure 6h), which was deeper than the temperature minimum layer. The water was thought to have originally been WCSW which obtained its low-N* signal from the shelf sediments. Because of the biological uptake of nutrients (e.g., silicate) in the shelf area in summer, the nutrient concentrations of the bottom shelf water were relatively low (Figure 6i). However, the bottom shelf water had high NO values, which were the same as those of the frTmin water around $S = 32.5$ in the Makarov Basin (Figure 6j). Therefore, the frTmin water was derived from the eastern part of the East Siberian Sea, rather than the western part of the sea. These results, and the fact that the frTmin water around $S = 32.5$ contained abundant oxygen (Figure 2h) and high f_{SIM} (Figure 4f), suggest that the WCSW containing a large amount of sea ice meltwater was cooled and oxygenated by winter convection in the eastern part of the East Siberian Sea. This water then flowed toward the Makarov Basin, resulting in the formation of a temperature minimum around $S = 32.5$ there.

3.5. Influence of Water Mass Changes in the Canada Basin

[27] The water mass changes west of the Chukchi Plateau would be transported into the Canada Basin through the ocean circulation. A drastic change west of the Chukchi Plateau was observed as the WCSW disappeared. Before and after modification by winter cooling and convection, this water was also characterized by the N* minimum around $S = 32.8$. Here we examine the horizontal distribution of N* on the isohaline surface of $S = 32.8$ and the ocean circulation at a depth of 100 m near the N* minimum (Figure 7). The ocean circulation was estimated from the dynamic height at 100 m relative to 250 m. The water flowed along contours of the dynamic height with higher values to the right.

[28] The flow patterns clearly suggested that changes in N* distribution were associated with changes in ocean circulation. In 2002, low-N* water seemed to spread from the East Siberian Sea into the Makarov Basin and then into the Canada Basin north of the Beaufort Gyre, expressed as closed contours of the dynamic height (north of 76°N at 150°W). The flow pattern and N* distribution in 2003 were similar to those in 2002, although no data are available for the Makarov Basin. In 2004, the Beaufort Gyre in the Canada Basin seemed to be slightly enhanced. The velocity evaluated from the gradient of dynamic height increased compared to that in 2002/2003, while low-N* water from the East Siberian Sea and/or the Chukchi Sea extended north of the Beaufort Gyre (north of 77°N at 150°W). In 2005–2007, low-N* water appeared north of the Beaufort Gyre, but we could not trace the origin of the water because of the lack of data west of 170°W. The Beaufort Gyre was largely enhanced in 2008–2010, and its area increased compared to that in previous years. In 2008, low-N* water from the East Siberian Sea no longer extended into the Canada Basin across the Chukchi Borderland. Along the shelf slope of the Chukchi Sea, low-N* water persistently appeared through 2002–2010. This low-N* water also came from the Chukchi Sea and may have been carried by an eastward flow located south of the westward flow of the Beaufort Gyre, along the shelf slope, as discussed by *Pickart* [2004], *Codispoti et al.* [2005], and *Hill and Cota* [2005].

[29] We used the location 79°N, 150°W, where data have been obtained every summer since 2003 and low-N* shelf water has been found up to 2007 (Figure 7), to monitor temporal changes in temperature and oxygen characteristics of the shelf water (Figure 8). This site was far from the formation region of eddies around the Chukchi Sea shelf slope, where eddies are produced by the baroclinic instability of shelf slope jets [*Pickart et al.*, 2005; *Kawaguchi et al.*, 2012]. Therefore, this site was assumed to be suitable for capturing the temporal changes in water masses rather than perturbations caused by eddies. In 2003, there was a prominent temperature maximum around $S = 32.5$, which is associated with WCSW (Figure 8a). The maximum temperature decreased in each successive year, and in 2007 the temperature profile had a minimum around $S = 32.3$ and a higher oxygen concentration than in previous years (Figure 8b). Therefore, this temperature minimum around $S = 32.3$ was probably formed by winter convection in the shelf area, as described above. Although it is difficult to estimate the time of year of the formation of this temperature minimum, it

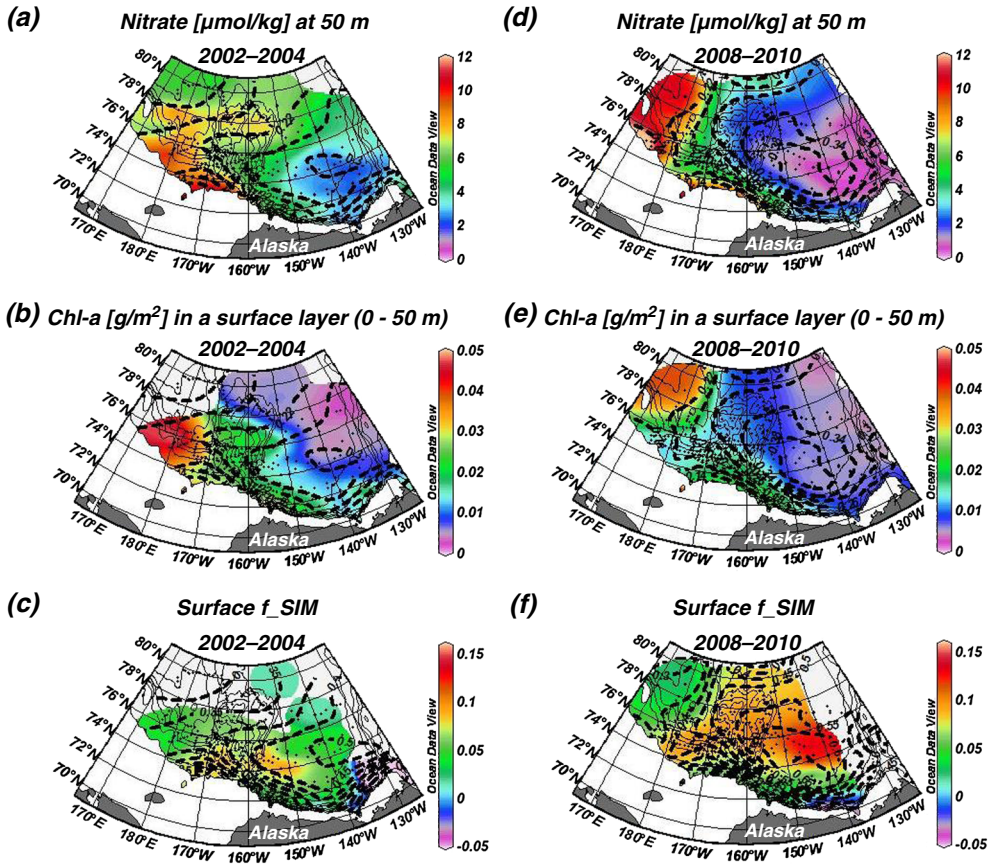

Figure 9. (a and d) Nitrate (µmol/kg) at 50 m and (b and e) CTD-Chl (g/m^2) in a layer from the surface to 50 m, and (c and f) f_{SIM} at the surface during 2002–2004 and 2008–2010, respectively. Dashed contours indicate dynamic height (dyn m) at 50 m relative to 250 m in Figures 9a, 9b, 9d, and 9e and at the surface relative to 250 m in Figures 9c and 9f.

might have been early winter when the ocean lost heat to the atmosphere (such as by cyclones) [e.g., *Inoue and Hori*, 2011] and was not yet covered by sea ice. In 2007, the WCSW at this location was replaced with water with this temperature minimum. In 2008, the temperature minimum appeared around $S = 33$, which is the typical temperature profile within the Beaufort Gyre in the Canada Basin. This is consistent with the fact that the Beaufort Gyre extended north of 79°N at 150°W after 2008. In the oxygen profile (Figure 8b), the oxygen minimum of water at $S = 32.8$ had a spike-like shape in 2003 and 2004, suggesting that the WCSW contacted the shelf sediments before it spread into the basin area. In 2005 and 2006, the oxygen minimum occurred in a broad range of salinities around $S = 33$. Although we do not know why this occurred, it is possible that the minimum may have been produced by the decomposition of organic matter not only at the bottom of the shelf where the WCSW passed but also at the bottom of the shelf slope occupied by water denser than the WCSW. In 2007, a small peak of high oxygen concentrations occurred around $S = 32.3$, which was probably influenced by the winter convection that produced the temperature-minimum water around $S = 32.3$ (Figure 8a). In the oxygen profile in 2008, the oxygen concentration around $S = 33$ was higher than that in previous years. This is because PWW ($S \sim 33$), which also experiences winter convection and has high oxygen concentrations, is carried into this location by the Beaufort Gyre. In 2003 and 2004, there was a temperature minimum and an oxygen maximum around $S = 33$, which are typical characteristics of the PWW. However, the circulation at the PWW level of 150 m (not shown) was similar to that at 100 m, indicating that this PWW originated from the west of the Chukchi Plateau, as did the WCSW. As shown in Figure 4, the PWW could extend to the west of the Chukchi Plateau even in 2002–2004. One question is why the PWW was not found at 79°N, 150°W, in 2005–2007. It is possible that the PWW did not extend to the west of the Chukchi Plateau in 2005–2007 and might have been replaced by the LHW with comparatively higher temperature and lower oxygen in that region.

3.6. Influence of Water Mass Changes on Biological Production

[30] The changes in ocean circulation could influence the biological production in the basin area, as discussed by *McLaughlin and Carmack* [2010] and *Nishino et al.* [2011b]. They suggested that biological production might decrease within the Beaufort Gyre in the Canada Basin, where the nutricline has deepened due to the accumulation of fresh water within the enhanced Beaufort Gyre [*Proshutinsky*

et al., 2009]. However, production might increase outside the gyre (such as in the Makarov Basin), where the nutricline has become shallower due to a large, nutrient-rich water input from the shelf, as described in this study. Because of limited data, previous studies did not examine the basin-scale Chl-a distribution. We combined data obtained during two periods: one was from 2002 to 2004 when the Beaufort Gyre was weak and small in extent, and the other was from 2008 to 2010 when the Beaufort Gyre was enhanced and larger (Figure 7). Here we examine the relationships among the distribution of Chl-a (CTD-Chl) in a layer above 50 m, which roughly corresponds to the euphotic zone, the nutrient (nitrate) distribution at 50 m, and the ocean circulation at 50 m (Figures 9a, 9b, 9d, and 9e). The relation between the Chl-a and surface sea ice meltwater distributions is also examined (Figures 9c and 9f).

[31] In 2002–2004, nutrient-rich water seemed to be carried by a northeastward flow from the East Siberian Sea into the Canada Basin north of the Beaufort Gyre via the Chukchi Abyssal Plain (Figure 9a). High Chl-a was found along this nutrient-rich water pathway (Figure 9b). This nutrient-rich water corresponded to frTmin water of $S \sim 32$ near a depth of 50 m (Figure 4b). As described in previous studies, the nutricline in the Canada Basin was shallower in the early 2000s than in the late 2000s. We further suggest that the shallow nutricline in 2002–2004 was maintained by the infusion of frTmin water with $S \sim 32$ and high nutrient concentration from the East Siberian Sea. This water may have sustained the high algal biomass in the Canada Basin.

[32] In 2008–2010, however, both the nutrient (Figure 9d) and Chl-a (Figure 9e) levels decreased from those in 2002–2004 in the Canada Basin, as described in previous studies. In contrast, in the Makarov Basin the nutrient concentration increased (Figure 9d) because of the shoaling of the nutricline. This was caused by a large-volume infusion of nutrient-rich frTmin water around $S = 32.5$, which was obtained from the shelf sediments before it spread into the basin. The shoaling of the nutricline may be favorable for phytoplankton growth in the Makarov Basin. The Chl-a distribution indicated that the Chl-a was indeed higher in the Makarov Basin than in the Canada Basin, but in the Makarov Basin the Chl-a decreased toward the shelf (Figure 9e). The Chl-a north of the East Siberian Sea was lower than that in 2002–2004. This might indicate that the biological production in this region was less in 2008–2010 than in 2002–2004, despite the shoaling of the nutricline. This result is the opposite of that obtained by *Nishino et al*. [2011b], who suggested an increase in biological production in the Makarov Basin accompanied by shoaling of the nutricline and improved light conditions resulting from sea ice loss. However, they only speculated based on the fact that the bottom nitrate concentration increased from 2002 to 2008, suggestive of an increase in organic matter deposition, decomposition, and remineralization as a result of increased biological production. In this region, north of the East Siberian Sea, why did the Chl-a decrease in 2008–2010 from that in 2002–2004, despite the increase in nutrients? Although the Chl-a distribution is primarily determined by the nutrient distribution, the surface sea ice meltwater may also influence the Chl-a distribution. The surface sea ice meltwater fraction f_{SIM} increased from 2002–2004 (Figure 9c) to 2008–2010 (Figure 9f) in both the Canada Basin and north of the East Siberian Sea. In 2008–2010, a large fraction of sea ice meltwater extended into the region north of the East Siberian Sea and may have decreased the Chl-a concentration. This is because the surface sea ice meltwater enhances the stratification of the water column and decreases the nutrient supply from lower layers, thereby leading to a reduction in the algal biomass.

4. Summary and Discussion

[33] The present study found that a temperature maximum of WCSW ($S = 32.5$) in the western Canada Basin and Makarov Basin disappeared in the late 2000s. In the late 2000s, a temperature minimum of $S = 32.5$ replaced the temperature maximum, with the temperature minimum water seeming to spread from the East Siberian Sea to the Makarov Basin. The temperature-minimum water around $S = 32.5$ has characteristics similar to WCSW (i.e., low N* and high f_{SIM}), but its oxygen concentration is much higher than that of WCSW, which has an oxygen minimum at $S = 32.8$. Therefore, WCSW with low N* and large amounts of sea ice meltwater, cooled and oxygenated by winter convection in the East Siberian Sea, resulted in the disappearance of the WCSW and the production of water at near-freezing temperature with high oxygen concentrations. The spreading of such shelf water into the Makarov Basin formed the temperature minimum around $S = 32.5$ in the basin.

[34] A water mass boundary that divides the waters from the east (Chukchi Sea) and west (East Siberian Sea) shifted from the Chukchi Plateau in the early 2000s to the Mendeleyev Ridge in the late 2000s. In the early 2000s, the frTmin water of $S \sim 32$ and WCSW of $S \sim 32.5$ were only found west of the Chukchi Plateau. A larger volume of PWW occupied the area to the east of the Chukchi Plateau than to its west. In the late 2000s, the frTmin water of $S \sim 32.5$, which was WCSW modified by cooling and convection, appeared west of the Mendeleyev Ridge. A large contribution of PWW penetrated westward of the ridge. Although the WCSW and its modified frTmin water were found in the Makarov Basin in the present study, *McLaughlin et al*. [1996] indicated that, based on the data obtained from CCGS *Henry Larsen* during summer 1993, Pacific-origin water was not found in the Makarov Basin. The Pacific/Atlantic front, which is characterized by the presence or absence of Pacific-origin water, was over the Mendeleyev Ridge at this time. Similarly, using data obtained from the cruise of the Arctic Ocean Section during summer 1994 [*Aagaard et al*., 1996; *Carmack et al*., 1997; *Swift et al*., 1997], *Shimada et al*. [2001] suggested that WCSW extended from the western Chukchi shelf slope to the eastern side of the Mendeleyev Ridge along the cruise section. The fragmented data coverage of these cruises in 1993 and 1994 might not capture the presence of Pacific-origin water in the Makarov Basin. Alternatively, the cyclonic regime of the Arctic Ocean circulation [*Proshutinsky and Johnson*, 1997] might have confined the Pacific-origin water to the east of the Mendeleyev Ridge [*McLaughlin et al*., 2002]. However, the anticyclonic regime has persisted since 1997 [*Proshutinsky et al*., 2011]. The Pacific/Atlantic front would therefore have moved to the Lomonosov Ridge [*McLaughlin et al*., 2002]. As a result, the WCSW and its modified frTmin water, which are of Pacific origin, were found in the Makarov Basin in the 2000s. In addition to the

anticyclonic regime of the Arctic Ocean circulation, which is controlled by the atmospheric circulation [*Proshutinsky and Johnson*, 1997], the recent loss of sea ice, which allows the wind to drive the ocean circulation more effectively, resulted in the enhancement of the Beaufort Gyre in the Canada Basin [*Shimada et al*., 2006; *Yang*, 2009]. Over the shelf slope north of the Chukchi and East Siberian seas, the westward flow of the Beaufort Gyre was also enhanced, and a strong westward flow along the shelf slope may have shifted the water mass boundary of frTmin water/WCSW and PWW from the Chukchi Plateau in the early 2000s to the Mendeleyev Ridge in the late 2000s.

[35] The sea ice distribution in October (the early freeze-up season) and the hydrographic data obtained from the East Siberian Sea suggest that the eastern part of the sea is the most plausible site for WCSW modification. After 2005, significant open water areas appeared in October in the eastern part of the East Siberian Sea. The cooling and convection in this area could form cold, thick, and oxygen-rich water, which would therefore have a high NO value. In the East Siberian Sea, cold waters, which would be formed by the above process in winter and remain until summer, occupied the bottom of the shelf. Their NO values were high in the eastern part but low in the western part. The frTmin water with $S \sim 32.5$ found in the Makarov Basin in 2008 had a high NO value like that found in the eastern part of the East Siberian Sea, suggesting a shared origin.

[36] The temporal changes in the temperature profiles at a station in the Canada Basin where shelf water with low N* arrived (Figure 8a) indicate that the temperature of WCSW gradually decreased from 2003 to 2006, and the temperature-minimum water appeared in 2007. However, the open water area in October in the eastern part of the East Siberian Sea, where the WCSW would be modified by cooling and convection, has drastically increased since 2005 (Figure 5b). The temperature of the WCSW should therefore have abruptly decreased after 2005 in this area. The gradual decrease in the WCSW temperature in the downstream area (the Canada Basin) suggests that the WCSW that was modified in each year in the eastern part of the East Siberian Sea did not directly flow into the Canada Basin, but instead mixed with other water and/or previously formed WCSW on its way to the Canada Basin. Such mixing would smooth the temperature decrease in the WCSW as it flowed downstream.

[37] The responses of ocean circulation, nutrient distribution, and biological activities to sea ice melting are quite different between the Canada and Makarov basins. The responses in the Canada Basin have already been studied by some researchers. In the Canada Basin, the Beaufort Gyre has recently become enhanced by the melting of thick, solid multi-year ice, which allows wind to more efficiently drive ocean circulation [*Shimada et al*., 2006; *Yang*, 2009]. An enhanced Beaufort Gyre increases the freshwater content in the Canada Basin [*Proshutinsky et al*., 2009]. The accumulation of fresh water and nutrient-poor surface waters can inhibit nutrient supply from deep layers and thus decrease phytoplankton production [*McLaughlin and Carmack*, 2010]. A quite different situation has occurred in the Makarov Basin. In recent years, the sea ice has retreated from the East Siberian Sea into the basin area in the winter freeze-up season, resulting in the formation of a large-volume water mass by cooling and convection. This water mass has high levels of nutrients obtained from the shelf sediments, and its infusion into the Makarov Basin makes the nutricline more shallow. Hence, because of this favorable nutrient availability for phytoplankton growth, phytoplankton biomass is prone to increase in areas where the sea ice disappears or becomes thin in summer, allowing light to penetrate the water for photosynthesis [*Nishino et al*., 2011b]. However, the sea ice meltwater has the effect of increasing the surface ocean stratification. This inhibits the nutrient supply from subsurface layers, resulting in a decrease in biological production. In the late 2000s, a large fraction of sea ice meltwater occupied not only the Beaufort Gyre in the Canada Basin but also the region north of the East Siberian Sea. In this region, the algal biomass became low compared with that in the early 2000s, despite the shoaling of the nutricline. If the more extensive melting of sea ice occurs, biological production in the Makarov Basin would be reduced, even with a shallow nutricline.

[38] **Acknowledgments.** The authors thank Koji Shimada, Eddy Carmack, and Fiona McLaughlin, who initiated and promoted the Japan-Canada collaborative project, Joint Western Arctic Climate Studies (JWACS), and Andrey Proshutinsky who led the Beaufort Gyre Exploration Project. The authors also thank the officers and crew of the R/V *Mirai* and CCGS *Louis S. St-Laurent*. The R/V *Mirai* was operated by Global Ocean Development, Inc., and skillful work and data processing aboard the ship were conducted by the staff of Marine Works Japan, Ltd. The work of I. S. and the ISSS-2008 cruise were supported by the NOAA OAR Climate Program Office (NA08OAR4600758), the Knut and Alice Wallenberg Foundation, the Swedish Polar Research Secretariat, the International Arctic Research Center of the University Alaska Fairbanks, and the Far Eastern Branch of Russian Academy of Sciences. Maps and figures were drawn using Ocean Data View software [*Schlitzer*, 2006].

References

Aagaard, K., L. K. Coachman, and E. Carmack (1981), On the halocline of the Arctic Ocean, *Deep-Sea Res.*, *28*, 529–545.

Aagaard, K., L. A. Bartie, E. C. Carmack, C. Garrity, E. P. Jones, D. Lubin, R. W. Macdonald, J. H. Swift, W. B. Tucker, P. A. Wheeler, and R. H. Whritner (1996), U.S., Canadian researchers explore Arctic Ocean, *Eos Trans. AGU*, *77*, 209–213.

Anderson, L. G., G. Björk, S. Jutterström, I. Pipko, N. Shakhova, I. Semiletov, and I. Wåhlström (2011), East Siberian Sea, an Arctic region of very high biogeochemical activity, *Biogeosciences*, *8*, 1745-1754, doi:10.5194/bg-8-1745-2011.

Broecker, W. S. (1974), "NO", a conservative water-mass tracer, *Earth Planet. Sci. Lett.*, *23*, 100–107.

Carmack, E. C., K. Aagaard, J. H. Swift, R. W. Macdonald, F. A. McLaughlin, E. P. Jones, R. G. Perkin, J. N. Smith, K. M. Ellis, and L. R. Killius (1997), Changes in temperature and tracer distributions within the Arctic Ocean: Results from the 1994 Arctic Ocean section, *Deep-Sea Res. II*, *44*, 1487–1502.

Coachman, L. K., and C. A. Barnes (1961), The contribution of Bering Sea water to the Arctic Ocean, *Arctic*, *14*, 147–161.

Coachman, L. K., K. Aagaard, and R. B. Tripp (1975), Bering Strait: The Regional Physical Oceanography, 172pp., Univ. of Wash. Press, Seattle, Wash.

Codispoti, L. A., and F. A. Richards (1968), Micronutrient distributions in the East Siberian and Laptev seas during summer 1963, *Arctic*, *21*, 67–83.

Codispoti, L. A., C. Flagg, V. Kelly, and J. H. Swift (2005), Hydrographic conditions during the 2002 SBI process experiments, *Deep-Sea Res. II*, *52*, 3199–3226.

Comiso, J. C., C. L. Parkinson, R. Gersten, and L. Stock (2008), Accelerated decline in the Arctic sea ice cover, *Geophys. Res. Lett.*, *35*, L01703, doi:10.1029/2007GL031972.

Devol, A. H., L. A. Codispoti, and J. P. Christensen (1997), Summer and winter denitrification rates in western Arctic shelf sediments, *Cont. Shelf Res.*, *17*, 1029–1050.

Dickson, A. G. (1996), Determination of dissolved oxygen in sea water by Winkler titration, in *WOCE Operations Manual*, Volume 3, Section 3.1, Part 3.1.3 WHP Operations and Methods, WHP Office Report WHPO 91-1, WOCE Report No. 68/91, Nov. 1994, Revision 1, 13pp., Woods Hole, Mass.

Gordon, L. I., J. C. Jennings, Jr., A. A. Ross, J. M. Krest (1993), A suggested protocol for continuous flow automated analysis of seawater nutrients (phosphate, nitrate, nitrite and silicic acid) in the WOCE Hydrographic Program and the Joint Global Ocean fluxes Study, in *WOCE Operations Manual*, Volume 3, Section 3.1, Part 3.1.3 WHP Operations

and Methods, WHP Office Report WHPO 91-1, WOCE Report No. 68/91, Nov. 1994, Revision 1, 55pp., Woods Hole, Mass.
Gruber, N., and J. L. Sarmiento (1997), Global patterns of marine nitrogen fixation and denitrification, *Global Biogeochem. Cycles*, *11* (2), 235–266.
Hansell, D. A., T. E. Whitledge, and J. J. Goering (1993), Patterns of nitrate utilization and new production over the Bering-Chukchi shelf, *Cont. Shelf Res.*, *13*, 601–627.
Haraldsson, C., L. G. Anderson, M. Hassellöv, S. Hulth, and K. Olsson (1997), Rapid, high-precision potentiometric titration of alkalinity in the ocean and sediment pore waters, *Deep-Sea Res. I*, *44*, 2031–2044.
Hill, V., and G. Cota (2005), Spatial patterns of primary production on the shelf, slope and basin of the Western Arctic in 2002, *Deep-Sea Res. II*, *52*, 3344–3354.
Inoue, J., and M. E. Hori (2011), Arctic cyclogenesis at the marginal ice zone: A contributory mechanism for the temperature amplification? *Geophys. Res. Lett.*, *38*, L12502, doi: 10.1029/2011GL047696.
Itoh, M. (2010), R/V Mirai Cruise Report MR10-05, www.godac.jamstec.go.jp/cruisedata/mirai/e/index.html, JAMSTEC, Yokosuka, Japan.
Itoh, M., E. Carmack, K. Shimada, F. McLaughlin, S. Nishino, and S. Zimmermann (2007), Formation and spreading of Eurasian source oxygen-rich halocline water into the Canadian Basin in the Arctic Ocean, *Geophys. Res. Lett.*, *34*, L08603, doi:10.1029/2007GL029482.
Jackson, J. M., E. C. Carmack, F. A. McLaughlin, S. E. Allen, and R. G. Ingram (2010), Identification, characterization, and change of the near-surface temperature maximum in the Canada Basin, 1993–2008, *J. Geophys. Res.*, *115*, C05021, doi:10.1029/2009JC005265.
Jones, E. P., and L. G. Anderson (1986), On the origin of the chemical properties of the Arctic Ocean halocline, *J. Geophys. Res.*, *91*, 10759–10767.
Kawaguchi, Y., M. Itoh, and S. Nishino (2012), Detailed survey of a large baroclinic eddy with extremely high temperatures in the Western Canada Basin, *Deep-Sea Res. I*, *66*, 90–102, doi:10.1016/j.dsr.2012.04.006.
Kikuchi, T. (2009), R/V Mirai Cruise Report MR09-03, 190 pp., JAMSTEC, Yokosuka, Japan.
Kwok, R., G. F. Cunningham, M. Wensnahan, H. J. Zwally, and D. Yi (2009), Thinning and volume loss of the Arctic Ocean sea ice cover: 2003–2008, *J. Geophys. Res.*, *114*, C07005, doi:10.1029/2009JC005312.
Markus, T., J. C. Stroeve, and J. Miller (2009), Recent changes in Arctic sea ice melt onset, freezeup, and melt season length, *J. Geophys. Res.*, *114*, C12024, doi:10.1029/2009JC005436.
McLaughlin, F. A., and E. C. Carmack (2010), Deepening of the nutricline and chlorophyll maximum in the Canada Basin interior, 2003–2009, *Geophys. Res. Lett.*, *37*, L24602, doi:10.1029/2010GL045459.
McLaughlin, F. A., E. C. Carmack, R. W. Macdonald, and J. K. B. Bishop (1996), Physical and geochemical properties across the Atlantic/Pacific water mass boundary in the southern Canadian Basin, *J. Geophys. Res.*, *101*, 1183–1197, doi:10.1029/95JC02634.
McLaughlin, F., E. Carmack, R. Macdonald, A. J. Weaver, and J. Smith (2002), The Canada Basin, 1989–1995: Upstream events and far-field effects of the Barents Sea, *J. Geophys. Res.*, *107*, 101,029–101,049, doi:10.1029/2001JC000904.
McLaughlin, F. A., E. C. Carmack, S. Zimmermann, D. Sieberg, L. White, J. Barwell-Clarke, M. Steel, and W. K. Li (2008), Physical and chemical data from the Canada Basin, August 2004, *Can. Data Rep. Hydrogr. Ocean Sci. 140*, Fish. and Oceans Can., Ottawa, Ont.
McLaughlin, F. A., et al. (2010), Physical, chemical and zooplankton data from the Canada Basin, August 2003, *Can. Data Rep. Hydrogr. Ocean Sci. 184*, Fish. and Oceans Can., Ottawa, Ont.
Nishino, S., K. Shimada, and M. Itoh (2005), Use of ammonium and other nitrogen tracers to investigate the spreading of shelf waters in the western Arctic halocline, *J. Geophys. Res.*, *110*, C10005, doi:10.1029/2003JC002118.
Nishino, S., K. Shimada, M. Itoh, M. Yamamoto-Kawai, and S. Chiba (2008), East-west differences in water mass, nutrient, and chlorophyll a distributions in the sea-ice reduction region of the western Arctic Ocean, *J. Geophys. Res.*, *113*, C00A01, doi:10.1029/2007JC004666.
Nishino, S., K. Shimada, M. Itoh, and S. Chiba (2009), Vertical double silicate maxima in the sea-ice reduction region of the western Arctic Ocean: Implications for an enhanced biological pump due to sea-ice reduction, *J. Oceanogr.*, *65*, 871-883, DOI 10.1007/s10872-009-0072-2.
Nishino, S., M. Itoh, Y. Kawaguchi, T. Kikuchi, and M. Aoyama (2011a), Impact of an unusually large warm-core eddy on distributions of nutrients and phytoplankton in the southwestern Canada Basin during late summer/early fall 2010, *Geophys. Res. Lett.*, *38*, L16602, doi:10.1029/2011GL047885.
Nishino, S., T. Kikuchi, M. Yamamoto-Kawai, Y. Kawaguchi, T. Hirawake, and M. Itoh (2011b), Enhancement/reduction of biological pump depends on ocean circulation in the sea-ice reduction regions of the Arctic Ocean, *J. Oceanogr.*, *67*, 305-314, DOI: 10.1007/s10872-011-0030-7.
Perovich, D. K., B. Light, H. Eicken, K. F. Jones, K. Runciman, and S. V. Nghiem (2007), Increasing solar heating of the Arctic Ocean and adjacent seas, 1979–2005: Attribution and role in the ice-albedo feedback, *Geophys. Res. Lett.*, *34*, L19505, doi:10.1029/2007GL031480.
Pickart, R. S. (2004), Shelfbreak circulation in the Alaskan Beaufort Sea: Mean structure and variability. *J. Geophys. Res. 109*, C04024, doi:10.1029/2003JC001912.
Pickart, R. S., T. J. Weingartner, L. J. Pratt, S. Zimmermann, and D. J. Torres (2005), Flow of winter-transformed Pacific water into the Western Arctic, *Deep Sea Res. II*, *52*, 3175–3198.
Proshutinsky, A. Y., and M. A. Johnson (1997), Two circulation regimes of the wind-driven Arctic Ocean, *J. Geophys. Res.*, *102*, 12,493–12,514, doi:10.1029/97JC00738.
Proshutinsky, A., R. Krishfield, M.-L. Timmermans, J. Toole, E. Carmack, F. McLaughlin, W. J. Williams, S. Zimmermann, M. Itoh, and K. Shimada (2009), Beaufort Gyre freshwater reservoir: State and variability from observations, *J. Geophys. Res.*, *114*, C00A10, doi:10.1029/2008JC005104.
Proshutinsky, A., et al. (2011), Ocean, the Arctic, in "state of the climate in 2010", edited by J. Blunden, D. S. Arndt, and M. O. Baringer, *Bull. Amer. Meteor. Soc.*, *92 (6)*, S145–S148.
Rudels, B., L. G. Anderson, and E. P. Jones (1996), Formation and evolution of the surface mixed layer and halocline of the Arctic Ocean, *J. Geophys. Res.*, *101*, 8807–8821.
Schlitzer, R. (2006), Ocean Data View, http://odv.awi.de.
Semiletov, I., and Ö. Gustafsson (2009), East Siberian Shelf Study alleviates scarcity of observations, *EOS*, *90*, 145–146.
Semiletov, I., O. Dudarev, V. Luchin, A. Charkin, K.-H. Shin, and N. Tanaka (2005), The East Siberian Sea as a transition zone between Pacific-derived waters and Arctic shelf waters, *Geophys. Res. Lett.*, *32*, L10614, doi:10.1029/2005GL022490.
Shimada, K. (2002), R/V Mirai Cruise Report MR02-K05 Leg1, edited by K. Shimada, S. Nishino, and M. Itoh, 226 pp., JAMSTEC, Yokosuka, Japan.
Shimada, K. (2004), R/V Mirai Cruise Report MR04-05, edited by K. Shimada, S. Nishino, and M. Itoh, 110 pp., JAMSTEC, Yokosuka, Japan.
Shimada, K. (2008), R/V Mirai Cruise Report MR08-04, 158 pp., JAMSTEC, Yokosuka, Japan.
Shimada, K., E. C. Carmack, K. Hatakeyama, and T. Takizawa (2001), Varieties of shallow temperature maximum waters in the western Canada Basin of the Arctic Ocean, *Geophys. Res. Lett.*, *28*, 3441–3444.
Shimada, K., M. Itoh, S. Nishino, F. McLaughlin, E. Carmack, and A. Proshutinsky (2005), Halocline structure in the Canada Basin of the Arctic Ocean, *Geophys. Res. Lett.*, *32*, L03605, doi:10.1029/2004GL021358.
Shimada, K., T. Kamoshida, M. Itoh, S. Nishino, E. Carmack, F. McLaughlin, S. Zimmermann, and A. Proshutinsky (2006), Pacific Ocean inflow: Influence on catastrophic reduction of sea ice cover in the Arctic Ocean, *Geophys. Res. Lett.*, *33*, L08605, doi:10.1029/2005GL025624.
Steele, M., J. Morison, W. Ermold, I. Rigor, M. Ortmeyer, and K. Shimada (2004), Circulation of summer Pacific halocline water in the Arctic Ocean, *J. Geophys. Res.*, *109*, C02027, doi:10.1029/2003JC002009.
Stroeve, J., M. M. Holland, W. Meier, T. Scambos, and M. Serreze (2007), Arctic sea ice decline: Faster than forecast, *Geophys. Res. Lett.*, *34*, L09501, doi:10.1029/2007GL029703.
Swift, J. H., E. P. Jones, K. Aagaard, E. C. Carmack, M. Hingston, R. W. Macdonald, F. A. McLaughlin, and R. G. Perkin (1997), Waters of the Makarov and Canada basins, *Deep-Sea Res. II*, *44*, 1503–1529.
UNESCO (1981), Background papers and supporting data on the Practical Salinity Scale, 1978, *UNESCO Technical Papers in Marine Science*, *37*, 1–144.
Weingartner, T. J., D. J. Cavalieri, K. Aagaard, and Y. Sasaki (1998), Circulation, dense water formation, and outflow on the northeast Chukchi shelf, *J. Geophys. Res.*, *103*, 7647–7661, doi:10.1029/98JC00374.
Welschmeyer, N.A. (1994), Fluorometric analysis of chlorophyll a in the presence of chlorophyll b and pheopigments, *Limnol. Oceanogr.*, *39*(8), 1985–1992.
Whitledge, T. E., W. S. Reeburgh, and J. J. Walsh (1986), Seasonal inorganic nitrogen distributions and dynamics in the southeastern Bering Sea, *Cont. Shelf Res.*, *5*, 109–132.
Wilson, C., and D. W. R. Wallace (1990), Using the nutrient ratio NO/PO as a tracer of continental shelf waters in the central Arctic Ocean, *J. Geophys. Res.*, *95*, 22,193-22,208.
Woodgate, R. A., K. Aagaard, J. H. Swift, W. M. Smethie, and K. K. Falkner (2002), Chukchi Borderland Cruise CBL2002 Arctic West-Phase II (AWS-02-II), University of Washington, Seattle, Wash.
Yamamoto-Kawai, M., N. Tanaka, and S. Pivovarov (2005), Freshwater and brine behaviors in the Arctic Ocean deduced from historical data of $\delta^{18}O$ and alkalinity (1929–2002 A.D.), *J. Geophys. Res.*, *110*, C10003, doi:10.1029/2004JC002793.
Yamamoto-Kawai, M., E. C. Carmack, and F. A. McLaughlin (2006), Nitrogen balance and Arctic throughflow, *Nature*, *443*, 43.
Yang, J. (2009), Seasonal and interannual variability of downwelling in the Beaufort Sea, *J. Geophys. Res.*, *114*, C00A14, doi:10.1029/2008JC005084.
Yao, W., and R. H. Byrne (1998), Simplified seawater alkalinity analysis: Use of linear array spectrometers, *Deep-Sea Res. I*, *45*, 1383–1392.